Received: 12 May 2016 | Revised: 28 July 2016 | Accepted: 12 August 2016
DOI 10.1111/cmi.12656

WILEY

RESEARCH ARTICLE

A pore-forming toxin enables *Serratia* a nonlytic egress from host cells

Gisela Di Venanzio† | **Martina Lazzaro**† | **Enrique S. Morales** | **Darío Krapf** | **Eleonora García Véscovi***

Instituto de Biología Molecular y Celular de Rosario, Consejo Nacional de Investigaciones Científicas y Tecnológicas, Universidad Nacional de Rosario, Rosario, Argentina

Correspondence
Eleonora García Véscovi, Instituto de Biología Molecular y Celular de Rosario, Consejo Nacional de Investigaciones Científicas y Tecnológicas, Universidad Nacional de Rosario, Ocampo y Esmeralda s/n, Predio CCT-CONICET-Rosario, 2000 Rosario, Argentina.
Email: garciavescovi@ibr-conicet.gov.ar

Abstract

Several pathogens co-opt host intracellular compartments to survive and replicate, and they thereafter disperse progeny to prosper in a new niche. Little is known about strategies displayed by *Serratia marcescens* to defeat immune responses and disseminate afterwards. Upon invasion of nonphagocytic cells, *Serratia* multiplies within autophagosome-like vacuoles. These *Serratia*-containing vacuoles (SeCV) circumvent progression into acidic/degradative compartments, avoiding elimination. In this work, we show that ShlA pore-forming toxin (PFT) commands *Serratia* escape from invaded cells. While ShlA-dependent, Ca^{2+} local increase was shown in SeCVs tight proximity, intracellular Ca^{2+} sequestration prevented *Serratia* exit. Accordingly, a Ca^{2+} surge rescued a ShlA-deficient strain exit capacity, demonstrating that Ca^{2+} mobilization is essential for egress. As opposed to wild-type-SeCV, the mutant strain-vacuole was wrapped by actin filaments, showing that ShlA expression rearranges host actin. Moreover, alteration of actin polymerization hindered wild-type *Serratia* escape, while increased intracellular Ca^{2+} reorganized the mutant strain-SeCV actin distribution, restoring wild-type-SeCV phenotype. Our results demonstrate that, by ShlA expression, *Serratia* triggers a Ca^{2+} signal that reshapes cytoskeleton dynamics and ends up pushing the SeCV load out of the cell, in an exocytic-like process. These results disclose that PFTs can be engaged in allowing bacteria to exit without compromising host cell integrity.

1 | INTRODUCTION

Serratia marcescens is an opportunistic human pathogen with reported increasing nosocomial infection incidence, and the cause of fatal outbreaks in neonatal intensive care units world-wide (Gastmeier, 2014; Schwab *et al*., 2014). *Serratia* can be the etiologic agent of meningitis, pneumonia, endocarditis, keratitis, osteomyelitis, urinary tract, and wound infections that can all progress to sepsis (Grimont & Grimont, 1978; Yu, 1979). Population-based studies showed that *Serratia* infections can also be community-acquired (Laupland *et al*., 2008; Parkins & Gregson, 2008). The emergence of *S. marcescens* as a threat to human health has been mainly attributed to multi-drug resistant strains emergence (Mahlen, 2011). Nevertheless, the underlying mechanisms that allow *Serratia* to surmount host defensive responses and the propagation and transmission strategies of this pathogen are still far from being elucidated.

We have previously demonstrated that *S. marcescens* is able to invade, survive, and proliferate inside nonphagocytic cells (Fedrigo, Campoy, Di Venanzio, Colombo, & Garcia Vescovi, 2011). Once inside the cell, *Serratia* inhabits and multiplies inside membrane-bound compartments that exhibit autophagic-like characteristics (Fedrigo *et al*., 2011). The vast majority of the SeCV population consists of nonacidic, nondegradative vesicles, indicating that *Serratia* is able to subvert the innate pathway of cellular elimination by counteracting the effect of SeCV fusion with lysosomal compartments (Fedrigo *et al*., 2011). Furthermore, the *phoPQ* mutant strain SeCV is preferentially delivered to acidic/degradative compartments, providing evidence that the PhoP/PhoQ two-component transduction system is implicated in the avoidance strategy that allows *Serratia* to survive and multiply intracellularly (Barchiesi, Castelli, Di Venanzio, Colombo, & Garcia Vescovi, 2012).

Cellular exit mechanisms are key stages for bacterial spread as they allow for disease progress and warrant a successful dispersal of the pathogen's progeny to new cells, tissues or hosts. Although not as deeply understood as internalization or intracellular survival

†These authors contributed equally to this work

 © 2016 John Wiley & Sons Ltd

strategies, bacterial egress processes so far described can be catalogued in lytic and nonlytic events for the host cell (Friedrich, Hagedorn, Soldati-Favre, & Soldati, 2012; Traven & Naderer, 2014). Processes that allow bacteria to be released from the invaded cell by promoting necroptosis, as reported for *Mycobacterium* and *Salmonella* (Robinson *et al*., 2012; Sridharan & Upton, 2014; Xu, Wang, Gao, & Liu, 2014), or pyroptosis, as is the case of *Legionella* and *Francisella* (Santic, Al-Khodor, & Abu Kwaik, 2010a; Santic, Pavokovic, Jones, Asare, & Kwaik, 2010b; Silveira & Zamboni, 2010) fall into lytic events. *Shigella* and *Listeria* are paradigms of pathogens that inflict extensive damage to the vacuolar membrane by expression of phospholipases and pore-forming toxin (PFT). However, once in the cytoplasm, they co-opt the function of cytoskeleton components to promote their egress by protrusion without cellular damage (Ireton, 2013; Kuehl, Dragoi, Talman, & Agaisse, 2015; Monack & Theriot, 2001). Other pathogens, such as *Porphyromonas gingivalis*, leave the cell redirecting the bacteria containing-vacuole to exocytic endosome recycling paths (Takeuchi, Furuta, & Amano, 2011) or within exosome-like structures, as is the case of uropathogenic *Escherichia coli* (Miao, Li, Zhang, Xu, & Abraham, 2015). Extrusion (Hybiske & Stephens, 2007) or ejection by induction of actin-based barrel-shaped structures (Hagedorn, Rohde, Russell, & Soldati, 2009) is also a nonlytic escape route that bypasses innate elimination responses.

Most bacteria-driven egress mechanisms engage the eukaryotic plasma membrane repair machinery (Beatty, 2007), the driving force of cytoskeleton components (Haglund & Welch, 2011), or are assisted by the autophagic pathway (Gerstenmaier *et al*., 2015; Hagedorn *et al*., 2009; Starr *et al*., 2012). Depending on environmental conditions or host cell types examined, a single pathogen often shows ability to exploit more than one of the aforementioned exit processes.

Several pathogen-secreted PFTs have been shown to be involved in the release of invading bacteria from the intracellular vacuole to the host cell cytoplasm due to their capacity to provoke disruption of membrane integrity (Alberti-Segui, Goeden, & Higgins, 2007; Alli *et al*., 2000; Bitar, Molmeret, & Kwaik, 2005; Gerstenmaier *et al*., 2015; Molmeret *et al*., 2002; Page, Ohayon, Sansonetti, & Parsot, 1999). Nonetheless, to our knowledge, no PFT has been identified as responsible for triggering a nonlytic escape of the host cell. In fact, in most cases, the identity of bacterial effectors responsible for manipulating the cellular physiology leading to egress and dissemination remains elusive.

One outstanding feature of *Serratia* consists in its ability to produce an array of secreted effectors that include lipases, proteases, chitinases, nucleases, and PFTs (Petersen & Tisa, 2013). Previous reports support the notion that the ShlA PFT is a key factor for *Serratia* pathogenic capacity (Di Venanzio, Stepanenko, & Garcia Vescovi, 2014; Fedrigo *et al*., 2011; Gonzalez-Juarbe *et al*., 2015a; Gonzalez-Juarbe *et al*., 2015b; Hertle, Hilger, Weingardt-Kocher, & Walev, 1999; Hertle & Schwarz, 2004; Marre, Hacker, & Braun, 1989; Lin *et al*., 2010). ShlA is encoded by the *shlBA* operon and, together with its translocator ShlB, constitutes a two-partner secretion system (Braun *et al*., 1987; Poole, Schiebel, & Braun, 1988; Hertle *et al*., 1999; Gonzalez-Juarbe *et al*., 2015b). *S. marcescens shlBA* mutant strains were found to be highly attenuated in infection models using *Caenorhabditis elegans* or *Drosophila melanogaster* (Kurz *et al*., 2003) and also in urinary tract (Marre *et al*., 1989) or in hemorrhagic pneumonia infection models in mice (Gonzalez-Juarbe *et al*., 2015b). Accordingly, ShlA overexpression provoked systemic infection and high mortality in pneumonia rat models (Lin *et al*., 2010).

In this work, we determine that, after intravacuolar replication, *Serratia* is able to promote its exit from the invaded epithelial cell. We identify ShlA as the bacterial factor required for the egress process to take place. In spite of being dependent on the expression of a PFT, *Serratia* exit strategy preserves the integrity of the host cell and shows mechanistic hallmarks of an exocytic process.

2 | RESULTS

2.1 | *Serratia* exits the invaded epithelial host cell in a ShlA-dependent process

After being internalized in the epithelial cell, the percentage of invaded cells was similar for either the wild-type or the *shlBA* mutant strain that does not express ShlA PFT, reaching 15.83 ± 2.01% for the wild-type and 12.94 ± 2.65%, at 120 min post infection (p.i.) (Figure 1a). We have previously shown that factors other than ShlA are responsible for the recruitment of the autophagic marker LC3 to the SeCV (Fedrigo *et al*., 2011; Di Venanzio *et al*., 2014) (hereafter also referred to as "wild-type-SeCV" as opposed to "*shlBA*-SeCV"). In addition, by performing a SeCV colocalization assay using EGFP-LC3-CHO cells and the lysosmotropic marker LysoTracker, we determined that up to 360 min p.i. either wild-type-SeCV or *shlBA*-SeCV consist in nonacidic vacuoles (Figure S1a and b and (Fedrigo *et al*., 2011)). These results indicate that ShlA expression is dispensable for early SeCV progression and for shaping the main features of the compartment where *Serratia* resides and proliferates intracellularly. Nevertheless, when CFU were analyzed after 120 min p.i., the *shlBA* mutant showed a 1.8 ± 0.4 (at 360 min p.i) or 4.6 ± 1.1 (at 480 min p.i.) -fold increase in the percentage of intracellular CFU values (relative to the inoculum), when compared to the wild-type strain (Figure 1b). A similar CFU pattern was obtained when T24 cells were invaded (Figure S2a), indicating that this differential phenotype is not restricted to a specific epithelial cell type. These results correlated with the microscopic inspection of SeCVs at 360 min p.i., being the ones containing the wild-type strain less crowded with bacteria than those harboring the *shlBA* strain (Figure 1c).

To verify that the lack of ShlA expression is responsible for the observed phenotype of the *shlBA* strain and because overexpression of *shlBA* from a plasmid renders an unregulated, high level expression of the PFT giving rise to artifacts, we tested a *shlB* mutant strain. The *shlB* strain does not express the ShlB transporter so it is unable to export ShlA, being nonhemolytic. The *shlB* strain was transformed with a plasmid bearing *shlB* (p*shlB*), which rescues ShlA export and thus restores the hemolytic phenotype (Figure S2b). As shown in Figure S2c, intracellular CFU scores for the *shlB* strain increased 2.6 ± 0.2-fold when compared to complemented *shlB*/p*shlB* strain, corroborating that ShlA expression is responsible for the differential intracellular CFU score observed between the wild-type and the *shlBA* strains shown in Figure 1b.

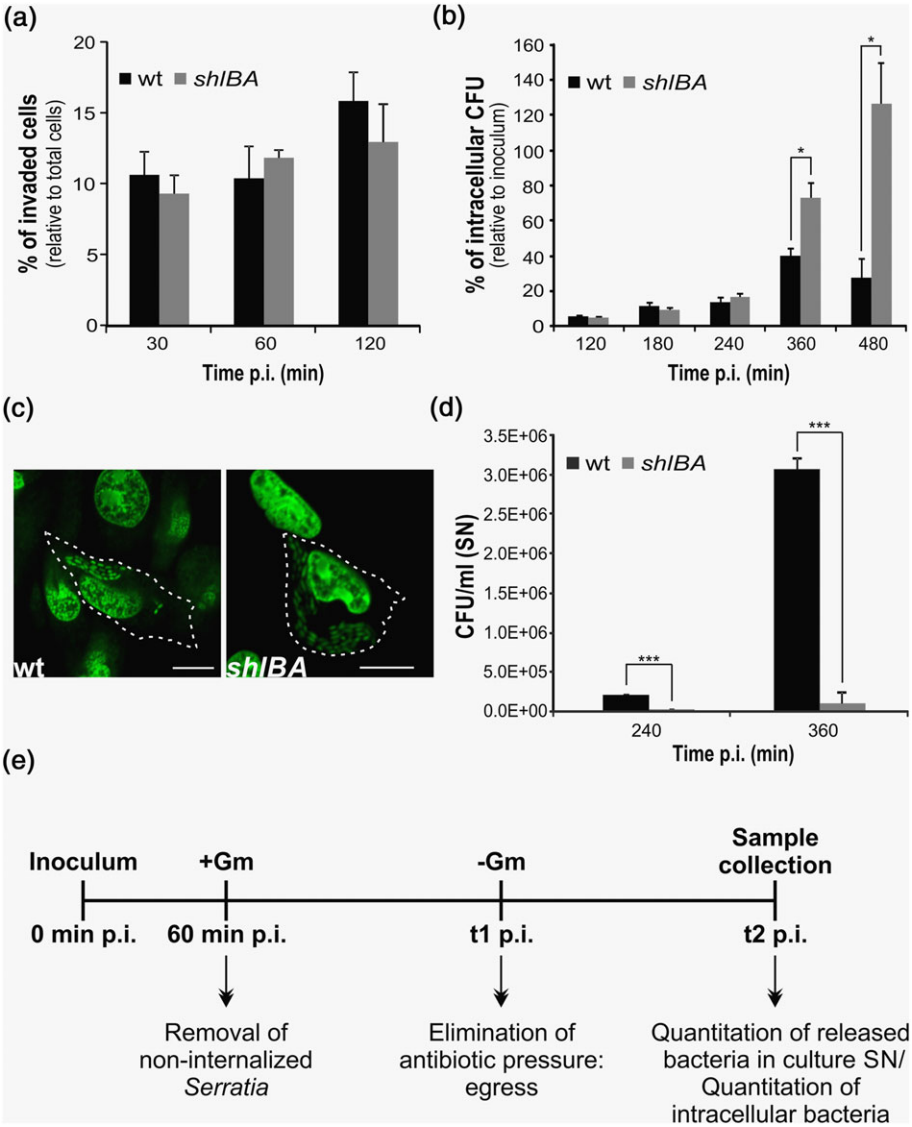

FIGURE 1 *Serratia* is able to escape from the eukaryotic cell in a ShlA-dependent manner. CHO cells were infected with the wild-type (wt) or *shlBA* strain at MOI = 10. (a) Cells were fixed at the indicated time points and detected by indirect immunofluorescence and differential permeabilization. Percentage of invasion was calculated as the total number of cells with intracellular bacteria relative to the total number of CHO cells. Three independent experiments were done by confocal microscopy and at least 300 cells were analyzed for each condition. Data represents means and S.D. (b) At the indicated times, intracellular CFU were determined. Percentage of intracellular CFU was calculated relative to the inoculum. The average ± S.D. for three independent experiments is shown (* $p < 0.05$). (c) Cells were stained with SYTO 9 (green fluorescence), fixed at 360 min p.i. and analyzed by confocal microscopy. Dashed lines indicate the cell border assessed from differential interference contrast (DIC) images. Bars: 10 μm. (d) After 180 or 240 min p.i., gentamicin was eliminated and replaced by free-antibiotic medium. CFU in supernatants per mL were determined at 240 or 360 min p.i., respectively. The average ± S.D. for three independent experiments is shown (** $p < 0.005$ and *** $p < 0.001$). SN: supernatant. (e) Scheme of the assay used to assess bacterial egress from CHO cells. Gm: gentamicin, t: time

The results presented above suggested either that *shlBA* strain was more proficient in intracellular replication than the wild-type strain or, that the wild-type strain was being eliminated more efficiently than the mutant one by the host cell. However, if after eliminating noninvading bacteria by gentamicin, the culture medium was replaced by antibiotic-free medium, the wild-type strain was found to be released to the culture supernatant. Wild-type strain CFU scores in the supernatant reached 5.7 ± 0.4-fold (at 240 min p.i.) or 30.4 ± 1.0-fold (at 360 min p.i.) higher values than those determined for the *shlBA* mutant (Figure 1d and e depicts the rationale of the assay used to assess bacterial egress from CHO cells). These results indicate that *Serratia* is able to escape from the eukaryotic intracellular niche, and that ShlA expression is required for the exit process to occur.

2.2 | *shlBA* transcription is enhanced intracellularly

To assess whether *shlBA* transcription was activated intracellularly, wild-type *Serratia* was transformed with pprom*shlBA-gfp*, a plasmid that contains a transcriptional fusion of *shlBA* promoter region to *gfp* (Di Venanzio *et al.*, 2014). The resulting strain showed an invasion behavior equivalent to the wild-type one (not shown). *gfp* expression levels were measured by flow cytometry at 120 and 360 min p.i. As shown in Figure S2d, *shlBA* transcription increased 1.79 ± 0.40 or

2.20 ± 0.32-fold at 120 or 360 min p.i., respectively, compared to the activity determined for bacteria in the inoculum. This result shows that *shlBA* transcription is induced after internalization into the host cell, consistent with a timely modulated ShlA expression required to promote *Serratia* egress.

2.3 | The egress of *Serratia* from the invaded cell is a nonlytic event

To monitor wild-type *Serratia* egress from the invaded CHO cells, time-lapse video microscopy was performed by using wild-type/p*gfp* labeled strain for the invasion assay. Both phase contrast and fluorescence images were acquired simultaneously at 30-s intervals using 488-nm excitation. Figure 2 and Movie S1 show the 352–360 min p.i. lapse when bacterial egress was detected. The video-microscopy shows that the complete bacterial load of the SeCV is released to the extracellular medium.

Next, we investigate whether, at the time when egress was overtly detected (360 min p.i.), *Serratia* affected the cytoplasmic membrane permeability properties or the viability of the invaded cell. With this aim, *in vivo* differential labeling with a membrane permeable dye (SYTO 9) and an impermeable one (propidium iodide) followed by microscopic quantification was performed. Out of 200 invaded cells analyzed, 100% were found to be stained by SYTO 9 fluorescence and no propidium iodide-labeled cells were found (Figure 3a). To rule out the possibility that damaged invaded cells that might have detached from the culture plate have been overlooked in the previous assay due to removal of the supernatant from the cell monolayer before the fixation step for imaging (see Experimental Procedures for details), after the invasion assay, viable versus nonviable cell populations were quantified by *in vivo* propidium iodide staining followed by flow cytometry, both in the attached monolayer and in the cell culture supernatant (Figure 3b). The controls consisted in CHO cells permeabilized with 0.1% Triton X-100 treatment or noninvaded, nontreated cells. No cells were detected in the culture supernatant while the presence of damaged (propidium iodide-stained) invaded cells was not detected in the attached layer. Moreover, no significant levels of lactate dehydrogenase (LDH) activity released to the extracellular medium were recovered from the invaded cell culture, reinforcing the previous result (Figure 3c). Furthermore, no evidence of altered cellular metabolic activity was obtained when it was tested by the tetrazolium dye 3-(4,5-dimethylthiazol-2-yl)-2,5-diphenyltetrazolium bromide (MTT) reduction assay, which measures NAD(P)H-dependent cellular oxidoreductase activity (Figure 3d). In sum, none of the above results revealed signals of plasma membrane integrity disruption or cell viability alteration, neither when the wild-type nor the *shlBA* strain were assayed. Collectively, these results indicate that *Serratia* is able to promote a ShlA-mediated, nonlytic egress from the invaded cell.

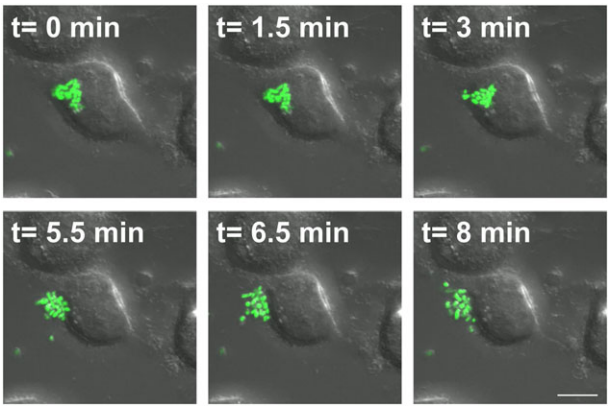

FIGURE 2 Images from time-lapse microscopy showing *wild-type Serratia* egress from the invaded CHO cell. CHO cells were invaded with wild-type/p*gfp* (green fluorescence). At 240 min p.i. cells were washed and FluoroBrite DMEM medium was added. Immediately, cells were visualized with a Zeiss LSM880 confocal microscope and images from 352 min p.i. (t = 0 min) to 360 min p.i. (t = 8 min) were analyzed with ImageJ software. Selected frames of merged DIC and fluorescence images of invaded CHO cells with time elapsed between frames are shown. Bars: 10 μm. The corresponding time-lapse movie showing *Serratia* egress is shown in Movie S1

2.4 | *Serratia* directs its exit from the host epithelial cell in an exocytic-like manner

In several exit mechanisms in which the pathogen-containing vacuole displays autophagosome-like features, the autophagic machinery was described to aid in the expulsion of the pathogen (Miao *et al.*, 2015; Ponpuak *et al.*, 2015). Therefore, we analyzed whether released bacteria from the invaded cells were surrounded by an accompanying eukaryotic membrane, and if this membrane was decorated with LC3 (the prototypic autophagy marker). No fluorescent LC3 positive staining colocalized with released bacteria from EGFP-LC3-CHO invaded cells (Figure S3). Additionally, as shown in Table S1, released bacteria were equally susceptible to gentamicin, with or without Triton X-100 pre-treatment, an assay previously designed to distinguish bacteria that exit enclosed in a eukaryotic cell-derived membrane (Miao *et al.*, 2015). These results show that egressed bacteria are not membrane encased. Taken together, the above shown results led us to hypothesize that *Serratia* egress could engage an exocytic-like mechanism.

It was previously established that, even in nonsecretory cells, an increase in intracellular free Ca^{2+} triggers exocytic mechanisms (Chieregatti & Meldolesi, 2005; Jaiswal, Andrews, & Simon, 2002). Therefore, to assess whether ShlA expression could induce mobilization of intracellular Ca^{2+}, Ca^{2+} levels were *in vivo* monitored with Fluo-3 AM, which exhibits an increase in fluorescence upon intracellular Ca^{2+} binding. Invaded CHO cells were loaded with Fluo-3 AM at 210 min p.i., and images were captured by confocal microscopy 30 min after. Fluo-3 AM fluorescent signal was detected juxtaposed to or colocalizing with 82.5% of wild-type-SeCV (Figure 4a, left panel). However, only 5.3% of *shlBA*-SeCV were detected in close association with a fluorescent Fluo-3 AM area (Figure 4a, right panel), discarding the possibility that high Fluo-3 AM signals were a consequence of Fluo-3 AM sub-compartmentalization. This result clearly demonstrated that intravacuolar *Serratia* is able to provoke a localized intracellular Ca^{2+} increase in a ShlA-dependent manner.

To gain further insight in this process, intracellular Ca^{2+} was sequestered to block exocytic events, and the effect on *Serratia* egress was analyzed. The fast membrane-permeant Ca^{2+} chelator BAPTA-AM

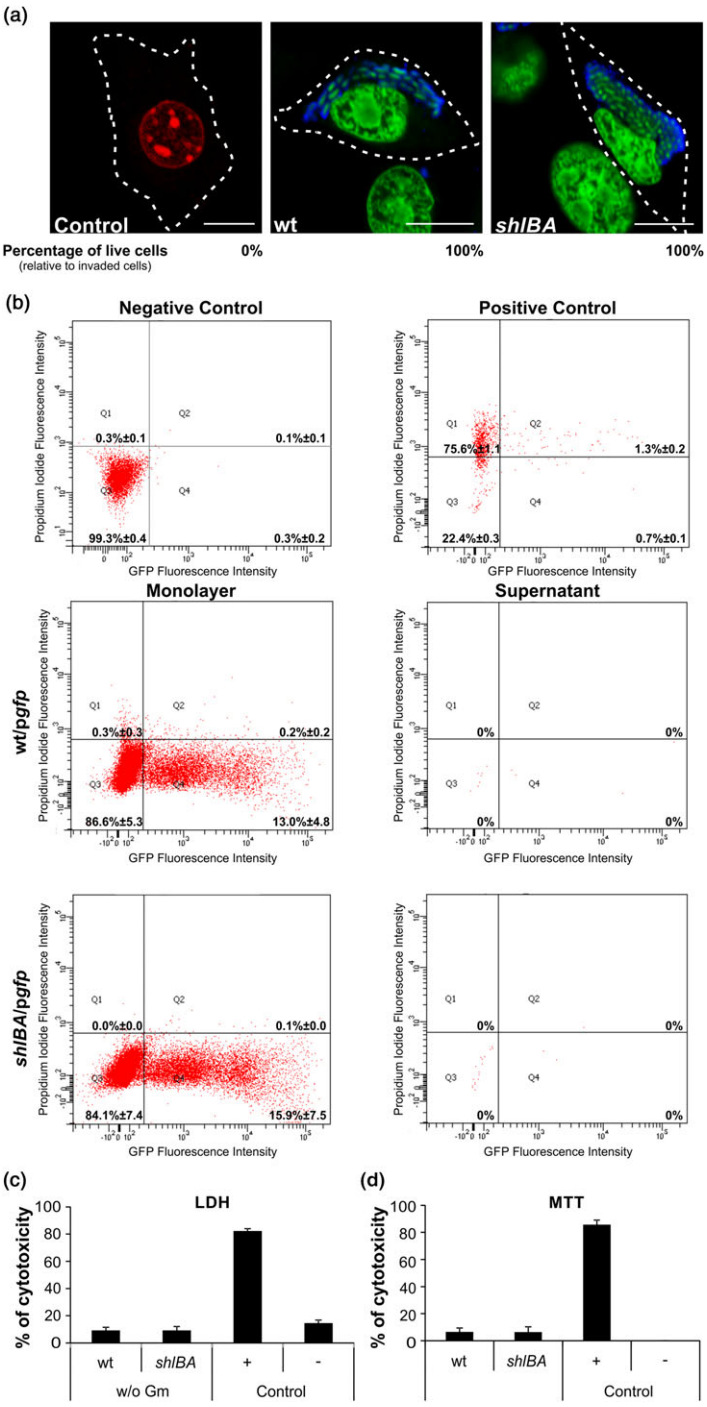

FIGURE 3 ShlA expression does not compromise the invaded cell viability. CHO cells were infected with wild-type (wt) or *shIBA* strain. (a) At 360 min p.i. cells were stained with the LIVE/DEAD Viability Kit (SYTO 9 green fluorescence, propidium iodide red fluorescence). Intracellular bacteria were detected by indirect immunofluorescence (blue fluorescence). Cells treated with Triton X-100 were included as controls. Representative confocal Z-slices are shown. At least 200 infected cells were monitored. Dashed lines indicate the cell border assessed from DIC images. Bars: 10 μm. Percentage of live, SYTO 9 stained, cells relative to total infected cells is shown at the bottom of each figure. (b) CHO cells were invaded with wild-type/p*gfp* (wt/p*gfp*) or *shIBA/pgfp*. At 360 min p.i., the cell culture supernatant and the cell monolayer were recovered, stained with propidium iodide (PI) and fixed. Samples were analyzed by FACSAria Cell Sorter. Cells treated with Triton X-100 were included as positive control and noninvaded cells were used as negative control. Signals in Q1 (high signal for PI and low signal for GFP) correspond to permeabilized noninvaded cells. Signals in Q2 (high signal for PI and high signal for GFP) correspond to permeabilized invaded cells. Signals in Q3 (low signal for PI and low signal for GFP) correspond to nonpermeabilized noninvaded cells. Signals in Q4 (low signal for PI and high signal for GFP) correspond to nonpermeabilized invaded cells. Percentages of each population were calculated relative to total cells. At least 30,000 cells were analyzed for each sample. The average ± S.D. for three independent experiments is shown. (c) LDH activity in the supernatant of infected CHO cells was measured at 360 mi p.i. Percentage of cytotoxicity was calculated as the activity of released LDH relative to total LDH activity (+: positive, −: negative controls). The average ± S.D. for five independent experiments is shown. (d) Infected CHO cells were washed and MTT was added at 360 min p.i. After incubation, violet formazan crystals were dissolved, and absorbance was read at λ = 570 nm (+: positive, −: negative controls). The average ± S.D. for five independent experiments is shown

was added to the CHO cells antibiotic-free culture medium at 240 min p.i. Both intracellular and extracellular released bacteria were enumerated at 360 min p.i. As shown in Figure 4b,c, when the wild-type strain was assayed, BAPTA-AM treatment increased 44% intracellular CFU, while it decreased 37% extracellular CFU, relative to nontreated cells. In contrast, when the *shIBA* strain was tested, differences in CFU were neither obtained for intracellular bacteria nor for bacteria recovered from the extracellular medium. Furthermore, to inhibit potential Ca^{2+} influx into the CHO cells, extracellular Ca^{2+} was sequestered by addition of EGTA to the culture medium. EGTA treatment inhibited 34% bacterial release in the wild-type strain and increased 60% intracellular CFU (Figure 4b,c), while no effect was observed for the *shIBA* strain, compared to nontreated cells. As shown in Figure S5a and b, the simultaneous addition of Ca^{2+} and EGTA in order to restore the free Ca^{2+} concentration levels found in the nontreated cell culture medium reverted the egress inhibition provoked by addition of EGTA alone. These results indicate that Ca^{2+} plays a critical role during the bacterial exit process.

We then reason that if ShlA-dependent intracellular Ca^{2+} mobilization triggered *Serratia* exocytic egress, mimicking an intracellular

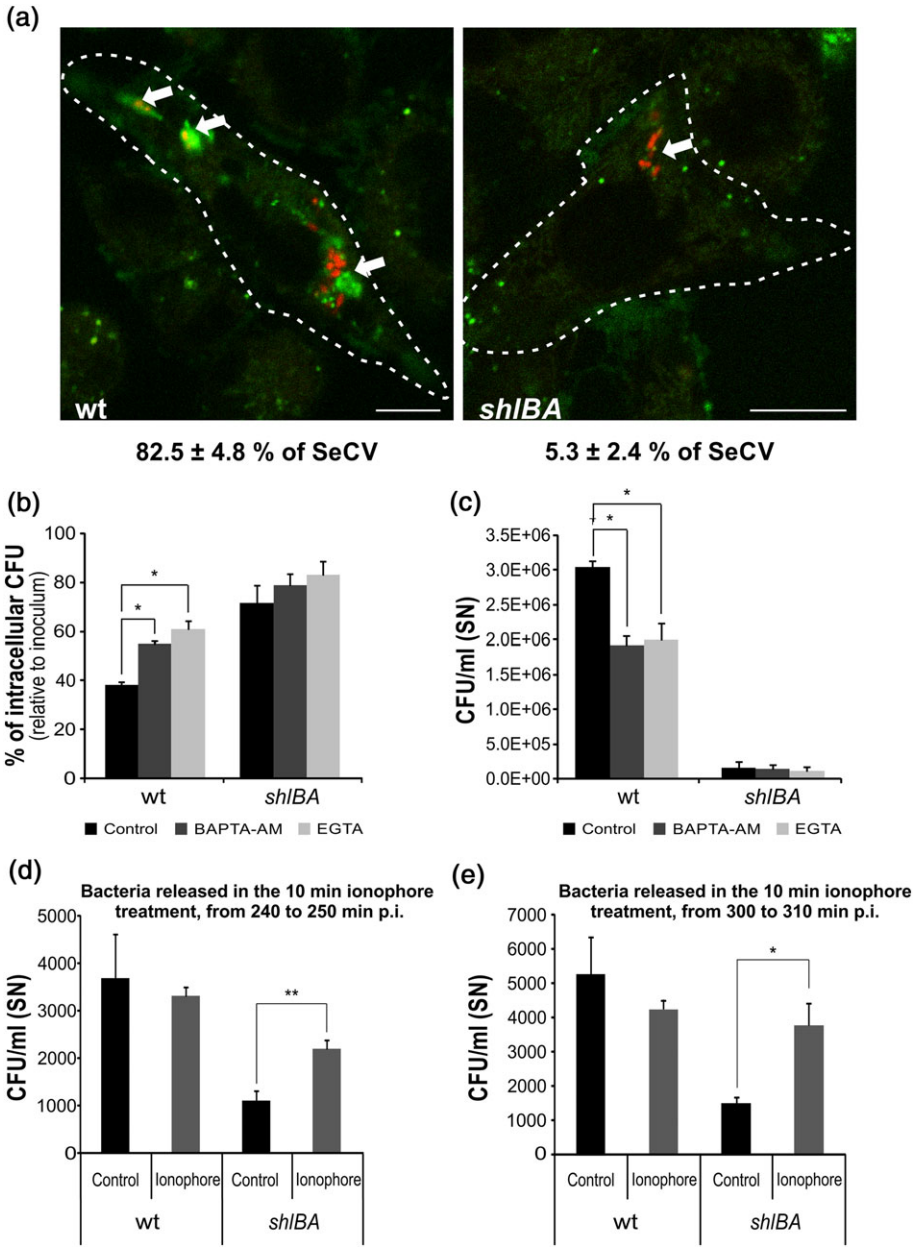

FIGURE 4 ShlA modulates intracellular Ca^{+2} mobilization to promote egress. (a) CHO cells were infected with wild-type/pmCherry (wt, red fluorescence) or *shlBA*/pmCherry (*shlBA*, red fluorescence). At 210 min p.i. Fluo-3 AM (green fluorescence) was added. Representative confocal laser microscopy images at 240 min p.i. are shown. Dashed lines indicate the cell border assessed from DIC images. Arrows point at SeCV. Bars: 10 μm. Percentage of localization of SeCV with fluorescent Fluo-3 AM, relative to total SeCV, is shown at the bottom of the figure. At least 200 infected cells were analyzed for each condition. The average ± S.D. for three independent experiments is shown. (b and c) CHO cells were infected with wild-type (wt) or *shlBA* strain. After 240 min, free-antibiotic medium with or without BAPTA-AM or EGTA was added. At 360 min p.i. (b) intracellular and (c) supernatant (SN) CFU were determined. Percentage of intracellular CFU was calculated relative to the inoculum and supernatant CFU were calculated per ml. The average ± S.D. for four independent experiments is shown (* $p < 0.05$ and ** $p < 0.01$). (d and e) CHO cells were infected with wild-type (wt) or *shlBA* strain. At (d) 240 or (e) 300 min p.i., free-antibiotic medium with or without ionophore A23187 was added. After 10-min incubation, CFU per mL in supernatants were determined. The average ± S.D. for four independent experiments is shown (* $p < 0.05$ and ** $p < 0.01$)

transient Ca^{2+} increase would lead to *Serratia* egress, even in the absence of ShlA. To this end, Ca^{2+} ionophore A23187 was used to pharmacologically increase intracellular Ca^{2+} concentration and induce exocytic events in the invaded CHO cells. At either 240 or 300 min p.i., gentamicin was removed from the culture medium, and ionophore A23187 was added. A23187 action was allowed for 10 min, and CFU recovered within this 10 min period were enumerated in the collected cell culture supernatant. Wild-type strain release was not affected by the ionophore treatment when compared to nontreated cells, while egress of the *shlBA* strain was increased by 97% (at 240 min p.i., Figure 4d) or 156% (at 300 min p.i., Figure 4e), in comparison to nontreated cells. Collectively, these results indicate that the intracellular Ca^{2+} surge promoted by the ionophore was able to bypass ShlA defect in the mutant strain, allowing for bacterial exit.

It has been demonstrated that an increase in intracellular Ca^{2+} suffices to stimulate lysosomal exocytosis in most cells, including the

CHO cell line (Rodriguez, Webster, Ortego, & Andrews, 1997). The release of the β-hexosaminidase enzyme, normally contained in the lysosomal cargo, was described to be a good marker for exocytic events (Rodriguez *et al.*, 1997). To verify the action of BAPTA-AM and ionophore A23187 on the exocytic mechanism of the cells, the release of the hexosaminidase was assayed by detecting its enzymatic activity using 4-methyl-umbellyferyl-N-acetyl-β-D-glucosaminide as substrate. α-Tubulin inmmunodetection was used as a control of the quantity of cells analyzed for the enzymatic assay. As shown in Figure S5c, the ionophore treatment increased 6.98-fold the hexosaminidase activity found in the cell culture supernatant, while BAPTA-AM treatment inhibited 0.52-fold hexosaminidase activity (Figure S5d). These results corroborate that Ca^{2+}-interfering drugs exerted the expected effects on CHO cells.

Taking into consideration that intracellular organelles are Ca^{2+} reservoirs (Jaiswal *et al.*, 2002), we next examined whether the SeCV membrane was altered in its permeability properties, which might be responsible for the localized Ca^{+2} increase observed associated to the wild-type-SeCV. β-Galactosides localize to the inner leaflet of vacuolar membranes, but get exposed to the cytosol upon vacuole damage. Due to its binding to exposed β-galactosides, Galectin-8 has proved to be a useful reporter for vacuolar membrane injury (Thurston, Wandel, von, Foeglein, & Randow, 2012). Therefore, a colocalization assay of SeCV with Galectin-8 was performed using CHO cells transiently expressing YFP-Gal8. While no significant difference in colocalization levels was detected at 120 or 240 min p.i., at 360 min p.i., Galectin-8 showed 2.5 ± 0.1-fold increased colocalization levels with the wild-type-SeCV, when compared to the value obtained for the mutant strain (Figure 5a and b; Figure S4 shows a series of Z-slices to provide further detail of the representative wild-type-SeCV shown in Figure 5b). This result indicates that *Serratia* is able to alter vacuolar permeability in a ShlA-dependent manner. It is important to note that, at this time p.i., the majority of wild-type SeCV analyzed were previously found to avoid the delivery to acidic/degradative compartments ((Fedrigo *et al.*, 2011) and also see Figure S1a and b), discarding the possibility that membrane damage might shuttle SeCV to host cell removal pathways.

In addition, an exocytic process would imply an active engagement of the cell cytoskeleton machinery, actin being a major player in both prefusion and postfusion vesicular motion events (Porat-Shliom, Milberg, Masedunskas, & Weigert, 2013). Therefore, actin distribution was examined in invaded CHO cells. Colocalization of actin filaments with SeCV was monitored by fluorescent phalloidin staining. While no difference in colocalization was observed between wild-type- and mutant-SeCV at 240 min p.i., *shlBA*-SeCV showed an average 2.81 ± 0.48-fold increase in colocalization values compared to wild-type-SeCV at 360 min p.i. (Figure 6a and b). In parallel, and to explore whether an intracellular Ca^{2+} mobilization was able to cause actin rearrangement associated to the SeCV, ionophore A23187 was added at 350 min p.i. and allowed 10 min for its action. This treatment reduced 3.7-fold the colocalization of *shlBA*-SeCV with actin while no significant changes were detected for wild-type-SeCV when compared to nontreated cells (Figure 6a and b). This result demonstrates that an increase in intracellular Ca^{2+} concentration is able to provoke a reorganization of actin filaments associated to the *shlBA*-SeCV, mirroring the wild-type-SeCV phenotype.

To assess if the differential actin engagement with the SeCV was relevant for the egress mechanism, polymerization of actin was pharmacologically prevented by addition of cytochalasin D (CD) at 240 min p.i. Extracellular CFU were then monitored at 360 min p.i. CD treatment reduced 53% the egress of the wild-type strain compared to the nontreated control. Unexpectedly, CD treatment enhanced 108% the egress of the *shlBA* mutant strain, compared to the nontreated control (Figure 6c).

These results together with those obtained by altering intracellular Ca^{2+} homeostasis allow us to conclude that ShlA intracellular expression promotes an increase in Ca^{2+} levels inside the invaded cell. This increase modulates actin-dependent cytoskeleton activity, provoking an exocytic process. In the absence of ShlA expression, the SeCV is coated by actin filaments and the bacterial exocytic process is precluded. However, ShlA action can be emulated either by inducing a transient increase in intracellular Ca^{2+} concentration or by altering actin dynamics.

3 | DISCUSSION

In this work, we demonstrate that, after actively replicating inside an intracellular vacuole within a nonphagocytic host cell, *S. marcescens* is able to direct its egress from within the invaded cell to the extracellular medium. We show that the expression of the ShlA PFT—which transcription is intracellularly induced—is essential for the exit process to occur. Accordingly, an otherwise isogenic mutant impaired in *shlBA* expression is retained within the SeCV, being unable to escape. We also show that viability and integrity of the host cell are preserved and that bacteria that reach the extracellular milieu are not encased in a host-cell-derived membrane, excluding an exosome-mediated exit.

It has been recognized that all, secretory and nonsecretory, eukaryotic cells exhibit constitutive exocytosis. This process is functional for protein delivery and for the repair and elongation of the plasma membrane (Chieregatti & Meldolesi, 2005). While in secretory cells, a variety of external signals are known to trigger Ca^{2+}-dependent exocytosis, recent evidences indicate that, even in nonsecretory cells, a free Ca^{2+} intracellular increase induces exocytic events. Whether the intracellular Ca^{2+} surge provokes exocytosis of vesicles already docked to the plasma membrane or induces the cytoskeleton activity, driving the vesicle movement to the fusion site and, at the same time, leading to dismantle localized cortical filamentous actin that stand in the way of vesicular docking at the membrane, is still a matter of debate (Miyake, McNeil, Suzuki, Tsunoda, & Sugai, 2001; Jaiswal *et al.*, 2002).

Our results showed that, at the time of egress, the wild-type strain, but not the *shlBA* mutant, was able to elicit a localized Ca^{2+} concentration increase in close proximity to the SeCV. Moreover, the PFT-mediated exit of wild-type *Serratia* could be mimicked by provoking a Ca^{2+} influx into the mutant strain invaded cell. On the other hand, an intracellular rise in Ca^{2+} concentration neither enhanced nor impeded the wild-type strain exit. Accordingly, sequestration of cytosolic Ca^{2+} hindered the exit process of the wild-type bacteria but had no effect on the inability of the *shlBA* strain to egress.

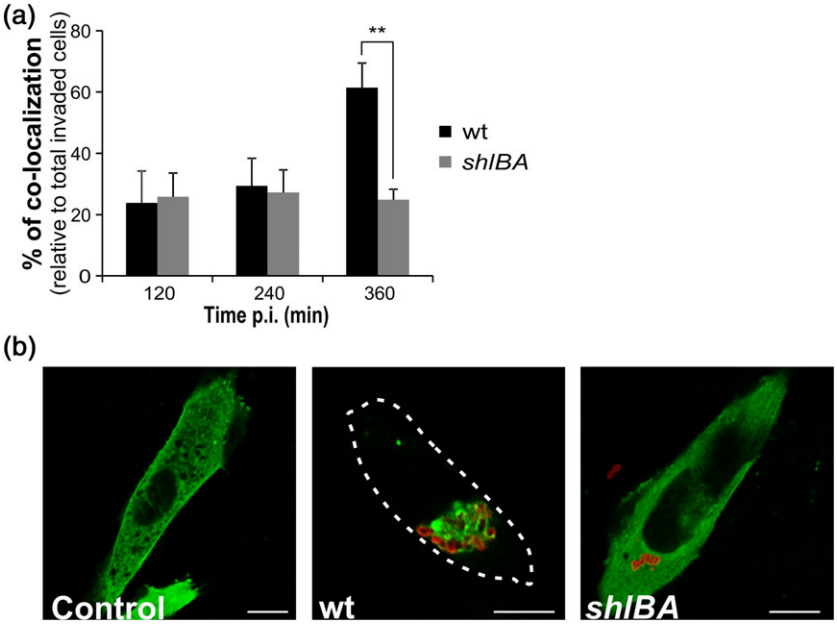

FIGURE 5 *Serratia* is able to alter vacuolar permeability in a ShlA-dependent manner. (a) CHO cells expressing YFP-Gal8 were infected with wild-type (wt) or *shlBA* strain. Cells were fixed at the indicated time points p.i., and bacteria were detected by indirect immunofluorescence. The percentage of colocalization of YFP-Gal8 with bacteria relative to total infected cells was determined by confocal microscopy. At least 200 infected cells were counted for each time point. The average ± S. D. for three independent experiments is shown (**$p < 0.01$). (b) Representative confocal laser images from the assay described in (a) are shown. CHO cells expressing YFP-Gal8 (green fluorescence) were infected with wild-type (wt) or *shlBA* strains (red fluorescence) and fixed at 360 min p.i. Noninfected cells are shown as control. Dashed lines indicate the cell border assessed from DIC images. Bars: 10 μm. A set of Z-slices depicting further details of the wild-type invaded cell are shown in Figure S4

Although extracellularly added EGTA provoked egress inhibition, suggesting that Ca^{2+} influx into the invaded cell might be the trigger of the bacterial exit, it has been previously demonstrated that buffering of Ca^{2+} out with EGTA rapidly depletes cytoplasmic Ca^{2+}, causing the arrest of intracellular Ca^{2+} oscillations from internal Ca^{2+} stores (Costello *et al.*, 2009), or the arrest of protein synthesis (Sotelo & Benech, 2013). Therefore, from our results, we are not able to discern whether the Ca^{2+} mobilization elicited by ShlA is intracellular or a result of Ca^{2+} influx. However, we favor the hypothesis that wild-type *Serratia* induces an intracellular mobilization of Ca^{2+} because: (a) BAPTA-AM, which chelates only intracellular Ca^{2+} inhibits bacterial egress, and (b) using Fluo3-AM we could detect an intracellular increase of Ca^{2+} locally associated to wild-type-SeCV but not with *shlBA*-SeCV. Besides, as intracellular vacuoles are Ca^{2+} storage compartments (Berridge, Bootman, & Roderick, 2003), it is tempting to speculate that ShlA-mediated alteration of the SeCV membrane permeability (as demonstrated by Galectin-8 recruitment) or, alternatively, the PFT insertion in the vacuolar membrane acting as a ionic channel or modulating the activity of Ca^{2+} vacuolar channels, could be responsible for Ca^{2+} efflux from the vacuole. Further work will be needed to assess the spatial and temporal location of ShlA production in connection to the Ca^{2+} intracellular mobilization.

Pharmacological inhibition of actin polymerization by cytochalasin D blocked ShlA-mediated exit, indicating that ShlA-dependent modulation of actin dynamics is directly linked to the exit process. Intriguingly, in contrast to the wild-type-SeCV, the *shlBA*-SeCV, which becomes anomalously enlarged by proliferation of the exit-impaired mutant, acquired a coating of filamentous actin, as demonstrated by positive phalloidin staining.

Recruitment of polymeric actin structures that wrap or entrap bacteria-containing vacuoles has been described for several pathogens with different outcomes. *Mycobacterium* recruits the actin nucleation-promoting factor WASH around the phagocytic vacuole, and this is shown to be implicated in the avoidance of fusion to lysosomal compartments (Kolonko *et al.*, 2014). *Chlamydia* co-opts the function of F-actin and intermediate filaments to structurally stabilize the inclusion with a dynamic scaffold that minimizes vacuole exposure to immune surveillance pathways (Kumar & Valdivia, 2008). In other pathogens, such as *Shigella*, initial actin recruitment leads the vacuole to an autophagy-mediated elimination (Haglund & Welch, 2011). Our results suggest that *Serratia* egress shares characteristics with *Cryptococcus neoformans* exit. In this fungus, actin polymerization cycles participate in the repair of a damaged pathogen-containing vacuole that will be finally expelled out of the cell. However, artificial stabilization of the actin polymers restricts the fungus exit, conceivably through steric inhibition of membrane fusion by the actin cage (Johnston & May, 2010).

In this context, two roles for actin in the *Serratia* exit process can be conceived: (a) it might dynamically polymerize and depolymerize around the SeCV in response to the intracellular Ca^{2+} signal promoted by ShlA expression, and (b) it can participate providing the force to drive SeCV exocytosis to completion via actin-based contractile activity that approaches the vacuole to the plasma membrane, pushing the docking-fusion events to take place (Porat-Shliom *et al.*, 2013). The nonphysiological, anomalous expansion of the *shlBA*-SeCV would place the actin-caged compartment in tight contact with the plasma membrane. In this situation, a pharmacologically induced dismantlement of the actin scaffold would suffice for the onset of an exocytic event. In addition, in the absence of ShlA expression, a provoked Ca^{2+} influx into the cytoplasm not only triggered the mutant strain egress but also promoted a redistribution of actin in the close proximity to the *shlBA*-SeCV, mimicking the wild-type-SeCV pattern. This result reinforces the notion of a link between ShlA-dependent intracellular Ca^{2+} signals and actin rearrangements within the host cell.

Altogether, our results indicate a mechanism in which ShlA induces an increase in intracellular Ca^{2+} that in turn activates actin dynamics. Subsequently, actin-mediated movement of cytoskeleton

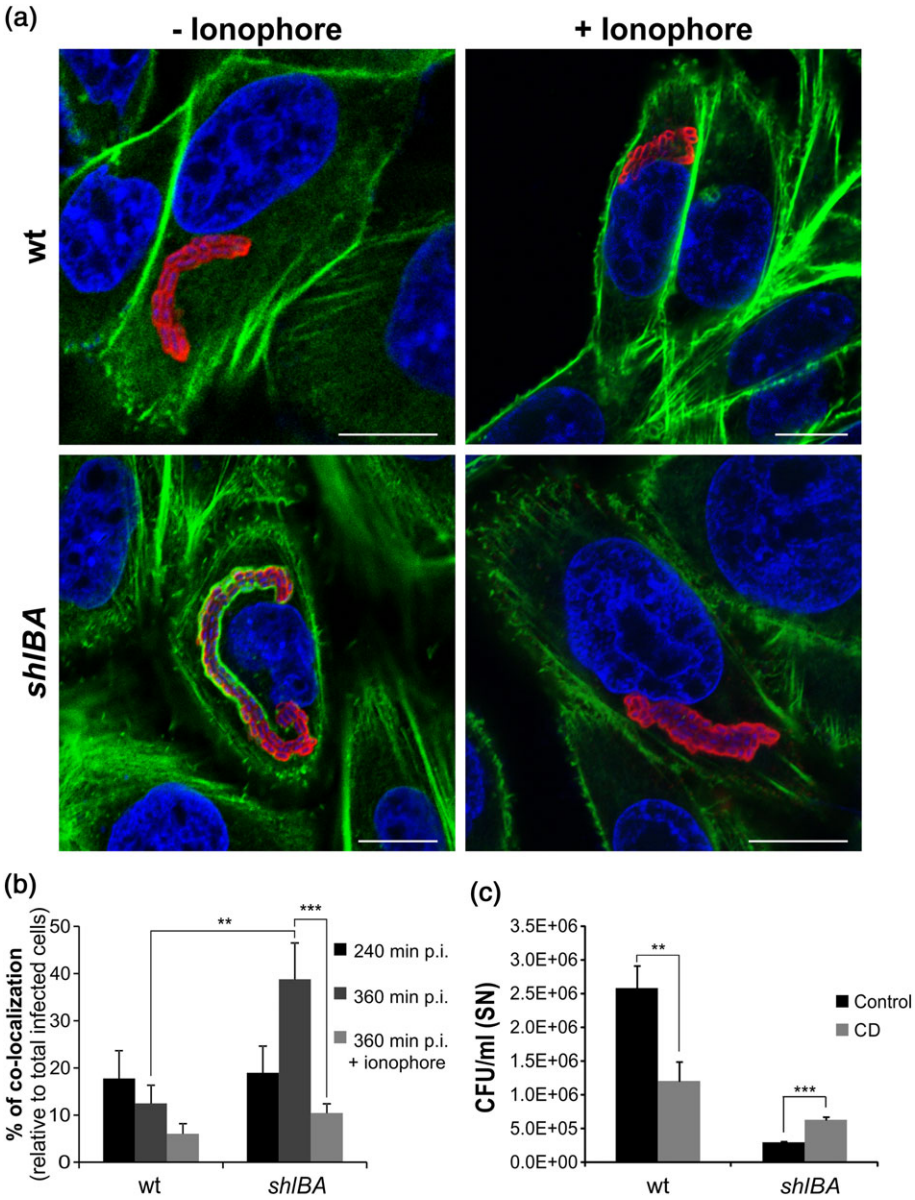

FIGURE 6 Actin dynamics is involved in bacterial egress and is affected by intracellular Ca^{2+} concentration. CHO cells were infected with wild-type (wt) or *shIBA* strain. At 350 min p.i., free-antibiotic medium with A23187 ionophore was added where indicated. At 240 and 360 min p.i., cells were fixed, intracellular bacteria and actin filaments were detected by indirect immunofluorescence. (a) Representative confocal Z-slices of CHO cells stained with Phalloidin-Alexa Fluor 488 (green fluorescence) and DAPI (blue fluorescence) infected with wild-type (wt) or *shIBA* strains (Cy3, red fluorescence), with or without ionophore treatment, at 360 min p.i. are shown. Bars: 10 μm. (b) At least 300 infected cells were analyzed by confocal microscopy for each condition and the percentage of colocalization was calculated as the ratio between the number of SeCV that colocalize with Phalloidin and the total number of infected cells. The average ± S.D. for three independent experiments is shown (** $p < 0.01$ and ***$p < 0.001$). (c) CHO cells were infected with wild-type (wt) or *shIBA* strain. After 240 min, free-antibiotic medium with or without cytochalasin D (CD) was added. At 360 min p.i. CFU in supernatants per ml were determined. The average ± S.D. for four independent experiments is shown (** $p < 0.01$ and *** $p < 0.001$)

components would propel the SeCV towards the plasma membrane where docking and fusion end in the exocytic discharge of the vesicle cargo to the extracellular medium.

In light of our results, the strong virulence attenuation previously demonstrated for *Serratia* strains unable to express ShlA using in vivo infection models (Kurz *et al.*, 2003; Hertle & Schwarz, 2004; Gonzalez-Juarbe *et al.*, 2015b; Marre *et al.*, 1989) can be attributed to their inability to successfully spread inside the host. We have determined that egressed *Serratia* collected from the host cells culture supernatant retain the ability to successfully invade naïve target cells (not shown). However, whether this escape mechanism endows the pathogen with the capacity to conquer new niches within a whole-animal host remains to be addressed.

In sum, our findings reveal that *Serratia* has developed a strategy to hijack the host cell vacuolar traffic and exit from the invaded epithelial cell, and point at ShlA as a critical target to fight against *Serratia* infections (Figure S6 depicts the *Serratia* egress mechanism herein proposed). They also underscore a novel role for a PFT, demonstrating that it can function as an intracellular effector able to trigger an exocytic, nonlytic bacterial escape from the invaded cell.

4 | EXPERIMENTAL PROCEDURES

4.1 | Bacterial strains and plasmids

The strains and plasmids used in this study are listed in Table S2.

4.1.1 | Construction of *shlBA* strain

A deletion of *shlBA* was constructed in the pES14 plasmid (Poole *et al.*, 1988). An internal fragment of the *shlBA* operon located between two HpaI restriction sites was replaced by a kanamycin resistance cassette (Kan^R). The 2.7-kb resulting fragment was cloned in the suicidal plasmid pKNG101 (Kaniga, Delor, & Cornelis, 1991) and conjugated into wild-type *S. marcescens* (Bruna, Revale, Garcia Vescovi, & Mariscotti, 2015). Mutant strains were selected as kanamycin-resistant and streptomycin-sensitive colonies. The *shlBA* deletion was confirmed by PCR and by phenotype analysis.

4.1.2 | Construction of p*shlB* plasmid

The *shlB* gene was cloned into EcoRI/BamHI-digested pBBR1MCS Cm^R plasmid (Kovach *et al.*, 1995). The resulting plasmid was mobilized into *shlB* mutant strain by conjugation.

4.2 | Gentamicin protection assay

The gentamicin protection assay was performed as described (Fedrigo *et al.*, 2011). All infection assays were done at multiplicity of infection (MOI) = 10 for CHO cells and at MOI = 2 for T24 cells. Percentage of intracellular CFU was calculated relative to the inoculum. To determine the number of bacteria in the extracellular medium of invaded cells, the gentamicin containing culture medium was replaced by free-antibiotic medium. At the indicated time points, the supernatant was recovered and serially diluted. CFU were determined on LB agar plates and CFU in supernatant per mL was calculated. The results for each experiment are the average of an assay performed in triplicate and independently repeated at least three times.

4.3 | Indirect immunofluorescence and confocal microscopy

To determine the percentage of infection at early time points, CHO cells infected with the wild-type or *shlBA* strain were fixed with 0.5 mL of 3% paraformaldehyde (PFA) solution in PBS for 10 min at the indicated time points. Cells were incubated with primary polyclonal antibodies against *S. marcescens* (1:500) and detected by incubation with anti-rabbit Cy3 conjugated secondary antibody (1:150). Cells were then permeabilized with 0.1% Triton X-100 in PBS for 10 min, incubated with primary polyclonal antibody anti-*S. marcescens* and detected by incubation with anti-rabbit Alexa Fluor 647-conjugated secondary antibody (1:300). Subsequently, cells were mounted with SlowFade Antifade reagent in glycerol/PBS. Percentage of invasion was calculated as the total number of cells with intracellular bacteria relative to the total number of CHO cells. Three independent experiments were done, and at least 300 cells were analyzed by confocal microscopy for each condition.

Infected cells expressing EGFP-LC3 or YFP-Gal8 were fixed with 0.5 mL of 3% PFA solution in PBS for 10 min and permeabilized with 0.1% Triton X-100 in PBS for 10 min. Subsequently, cells were incubated with primary polyclonal antibody against *S. marcescens* and detected by incubation with anti-rabbit Cy3 conjugated secondary antibody (red fluorescence) or anti-rabbit Alexa Fluor 647-conjugated secondary antibodies (blue fluorescence). Cells were mounted with SlowFade Antifade reagent in glycerol/PBS. Cells were analyzed by confocal microscopy with a Nikon Eclipse TE-2000-E2 and the EZ-C1 3.20 Free Viewer program (Nikon, Japan). The percentage of colocalization was calculated as the ratio between the number of vesicles containing bacteria that colocalize with the indicated fluorescently labeled marker and the total number of infected cells or the total number of SeCV, as indicated.

4.4 | Statistical analysis

Statistical analysis was performed using one-way ANOVA and Tukey-Kramer Multiple Comparisons test with an overall significance level = 0.05. Asterisks in the plots denote the values among the treatment groups in which a statistical significant difference was determined.

4.5 | See SI for additional Experimental Procedures

ACKNOWLEDGMENTS

We are grateful to R. Vena (confocal laser microscopy), M. Ojeda (flow cytometry), D. Campos (tissue culture), and M. Avecilla for excellent technical assistance; to M. I. Colombo, A. Cáceres, C. Fader, and R. Rodriguez for advice, F. C. Soncini for critically reading the manuscript, V. Braun and S. I. Patzer for providing pES14, M. F. Feldman, C. Larocca, E.C. Serra, and D. Ferrandon for the kind gift of reagents. EGV and DK are career investigators of Consejo de Investigaciones Científicas y Tecnológicas (CONICET), Argentina. GDV and ML have fellowships from CONICET and from Agencia Nacional de Promoción Científica y Tecnológica (ANPCyT), Argentina. This work was supported by a grant from ANPCyT, PICT 2012-1403, to EGV. The funders had no role in study design, data collection and interpretation, or the decision to submit the work for publication.

REFERENCES

Alberti-Segui, C., Goeden, K. R., & Higgins, D. E. (2007). Differential function of *Listeria monocytogenes* listeriolysin O and phospholipases C in vacuolar dissolution following cell-to-cell spread. *Cellular Microbiology*, *9*, 179–195.

Alli, O. A., Gao, L. Y., Pedersen, L. L., Zink, S., Radulic, M., Doric, M., & Abu Kwaik, Y. (2000). Temporal pore formation-mediated egress from macrophages and alveolar epithelial cells by *Legionella pneumophila*. *Infection and Immunity*, *68*, 6431–6440.

Barchiesi, J., Castelli, M. E., Di Venanzio, G., Colombo, M. I., & Garcia Vescovi, E. (2012). The PhoP/PhoQ system and its role in *Serratia marcescens* pathogenesis. *Journal of Bacteriology*, *194*, 2949–2961.

Beatty, W. L. (2007). Lysosome repair enables host cell survival and bacterial persistence following *Chlamydia trachomatis* infection. *Cellular Microbiology*, *9*, 2141–2152.

Berridge, M. J., Bootman, M. D., & Roderick, H. L. (2003). Calcium signalling: Dynamics, homeostasis and remodelling. *Nature Reviews. Molecular Cell Biology*, *4*, 517–529.

Bitar, D. M., Molmeret, M., & Kwaik, Y. A. (2005). Structure–function analysis of the C-terminus of IcmT of *Legionella pneumophila* in pore formation-mediated egress from macrophages. *FEMS Microbiology Letters*, *242*, 177–184.

Braun, V., Neuss, B., Ruan, Y., Schiebel, E., Schoffler, H., & Jander, G. (1987). Identification of the *Serratia marcescens* hemolysin determinant by cloning into *Escherichia coli*. *Journal of Bacteriology*, *169*, 2113–2120.

Bruna, R. E., Revale, S., Garcia Vescovi, E., & Mariscotti, J. F. (2015). Draft whole-genome sequence of *Serratia marcescens* strain RM66262, isolated from a patient with a urinary tract infection. *Genome Announcement*, *3*, pii: e014237-15.

Chieregatti, E., & Meldolesi, J. (2005). Regulated exocytosis: New organelles for non-secretory purposes. *Nature Reviews. Molecular Cell Biology*, *6*, 181–187.

Costello, S., Michelangeli, F., Nash, K., Lefievre, L., Morris, J., Machado-Oliveira, G., … Publicover, S. (2009). Ca2+-stores in sperm: Their identities and functions. *Reproduction*, *138*, 425–437.

Di Venanzio, G., Stepanenko, T. M., & Garcia Vescovi, E. (2014). *Serratia marcescens* ShlA pore-forming toxin is responsible for early induction of autophagy in host cells and is transcriptionally regulated by RcsB. *Infection and Immunity*, *82*, 3542–3554.

Fedrigo, G. V., Campoy, E. M., Di Venanzio, G., Colombo, M. I., & Garcia Vescovi, E. (2011). *Serratia marcescens* is able to survive and proliferate in autophagic-like vacuoles inside non-phagocytic cells. *PloS One*, *6*, . e24054.

Friedrich, N., Hagedorn, M., Soldati-Favre, D., & Soldati, T. (2012). Prison break: Pathogens' strategies to egress from host cells. *Microbiology and Molecular Biology Reviews*, *76*, 707–720.

Gastmeier, P. (2014). *Serratia marcescens*: An outbreak experience. *Frontiers in Microbiology*, *5*, 81.

Gerstenmaier, L., Pilla, R., Herrmann, L., Herrmann, H., Prado, M., Villafano, G. J., … Hagedorn, M. (2015). The autophagic machinery ensures nonlytic transmission of mycobacteria. *Proceedings of the National Academy of Sciences of the United States of America*, *112*, E687–E692.

Gonzalez-Juarbe, N., Gilley, R. P., Hinojosa, C. A., Bradley, K. M., Kamei, A., Gao, G., … Orihuela, C. J. (2015a). Pore-forming toxins induce macrophage necroptosis during acute bacterial pneumonia. *PLoS Pathogens*, *11*, .e1005337.

Gonzalez-Juarbe, N., Mares, C. A., Hinojosa, C. A., Medina, J. L., Cantwell, A., Dube, P. H., … Bergman, M. A. (2015b). Requirement for *Serratia marcescens* cytolysin in a murine model of hemorrhagic pneumonia. *Infection and Immunity*, *83*, 614–624.

Grimont, P. A., & Grimont, F. (1978). The genus Serratia *Annu. Review Microbioliology*, *32*, 221–248.

Hagedorn, M., Rohde, K. H., Russell, D. G., & Soldati, T. (2009). Infection by tubercular mycobacteria is spread by nonlytic ejection from their amoeba hosts. *Science*, *323*, 1729–1733.

Haglund, C. M., & Welch, M. D. (2011). Pathogens and polymers: Microbe–host interactions illuminate the cytoskeleton. *The Journal of Cell Biology*, *195*, 7–17.

Hertle, R., & Schwarz, H. (2004). *Serratia marcescens* internalization and replication in human bladder epithelial cells. *BMC Infectious Diseases*, *4*, 16.

Hertle, R., Hilger, M., Weingardt-Kocher, S., & Walev, I. (1999). Cytotoxic action of *Serratia marcescens* hemolysin on human epithelial cells. *Infection and Immunity*, *67*, 817–825.

Hybiske, K., & Stephens, R. S. (2007). Mechanisms of host cell exit by the intracellular bacterium Chlamydia. *Proceedings of the National Academy of Sciences of the United States of America*, *104*, 11430–11435.

Ireton, K. (2013). Molecular mechanisms of cell–cell spread of intracellular bacterial pathogens. *Open Biology*, *3*, .130079. DOI: 10.1098/rsob.130079 Review.

Jaiswal, J. K., Andrews, N. W., & Simon, S. M. (2002). Membrane proximal lysosomes are the major vesicles responsible for calcium-dependent exocytosis in nonsecretory cells. *The Journal of Cell Biology*, *159*, 625–635.

Johnston, S. A., & May, R. C. (2010). The human fungal pathogen *Cryptococcus neoformans* escapes macrophages by a phagosome emptying mechanism that is inhibited by Arp2/3 complex-mediated actin polymerisation. *PLoS Pathogens*, *6*, .e1001041.

Kaniga, K., Delor, I., & Cornelis, G. R. (1991). A wide-host-range suicide vector for improving reverse genetics in gram-negative bacteria: Inactivation of the blaA gene of *Yersinia enterocolitica*. *Gene*, *109*, 137–141.

Kolonko, M., Geffken, A. C., Blumer, T., Hagens, K., Schaible, U. E., & Hagedorn, M. (2014). WASH-driven actin polymerization is required for efficient mycobacterial phagosome maturation arrest. *Cellular Microbiology*, *16*, 232–246.

Kovach, M. E., Elzer, P. H., Hill, D. S., Robertson, G. T., Farris, M. A., Roop, R. M. 2nd, & Peterson, K. M. (1995). Four new derivatives of the broad-host-range cloning vector pBBR1MCS, carrying different antibiotic-resistance cassettes. *Gene*, *166*, 175–176.

Kuehl, C. J., Dragoi, A. M., Talman, A., & Agaisse, H. (2015). Bacterial spread from cell to cell: Beyond actin-based motility. *Trends in Microbiology*, *23*, 558–566.

Kumar, Y., & Valdivia, R. H. (2008). Actin and intermediate filaments stabilize the *Chlamydia trachomatis* vacuole by forming dynamic structural scaffolds. *Cell Host & Microbe*, *4*, 159–169.

Kurz, C. L., Chauvet, S., Andres, E., Aurouze, M., Vallet, I., Michel, G. P., … Ewbank, J. J. (2003). Virulence factors of the human opportunistic pathogen *Serratia marcescens* identified by in vivo screening. *The EMBO Journal*, *22*, 1451–1460.

Laupland, K. B., Parkins, M. D., Gregson, D. B., Church, D. L., Ross, T., & Pitout, J. D. (2008). Population-based laboratory surveillance for Serratia species isolates in a large Canadian health region. *European Journal of Clinical Microbiology & Infectious Diseases*, *27*, 89–95.

Lin, C. S., Horng, J. T., Yang, C. H., Tsai, Y. H., Su, L. H., Wei, C. F., … Lai, H. C. (2010). RssAB-FlhDC-ShlBA as a major pathogenesis pathway in *Serratia marcescens*. *Infection and Immunity*, *78*, 4870–4881.

Mahlen, S. D. (2011). Serratia infections: From military experiments to current practice. *Clinical Microbiology Reviews*, *24*, 755–791.

Marre, R., Hacker, J., & Braun, V. (1989). The cell-bound hemolysin of *Serratia marcescens* contributes to uropathogenicity. *Microbial Pathogenesis*, *7*, 153–156.

Miao, Y., Li, G., Zhang, X., Xu, H., & Abraham, S. N. (2015). A TRP channel senses lysosome neutralization by pathogens to trigger their expulsion. *Cell*, *161*, 1306–1319.

Miyake, K., McNeil, P. L., Suzuki, K., Tsunoda, R., & Sugai, N. (2001). An actin barrier to resealing. *Journal of Cell Science*, *114*, 3487–3494.

Molmeret, M., Alli, O. A., Zink, S., Flieger, A., Cianciotto, N. P., & Kwaik, Y. A. (2002). icmT is essential for pore formation-mediated egress of *Legionella pneumophila* from mammalian and protozoan cells. *Infection and Immunity*, *70*, 69–78.

Monack, D. M., & Theriot, J. A. (2001). Actin-based motility is sufficient for bacterial membrane protrusion formation and host cell uptake. *Cellular Microbiology*, *3*, 633–647.

Page, A. L., Ohayon, H., Sansonetti, P. J., & Parsot, C. (1999). The secreted IpaB and IpaC invasins and their cytoplasmic chaperone IpgC are required for intercellular dissemination of *Shigella flexneri*. *Cellular Microbiology*, *1*, 183–193.

Parkins, M. D., & Gregson, D. B. (2008). Community-acquired *Serratia marcescens* spinal epidural abscess in a patient without risk factors: Case report and review. *Canadian Journal of Infectious Diseases and Medical Microbiology*, *19*, 250–252.

Petersen, L. M., & Tisa, L. S. (2013). Friend or foe? A review of the mechanisms that drive Serratia towards diverse lifestyles. *Canadian Journal of Microbiology*, *59*, 627–640.

Ponpuak, M., Mandell, M. A., Kimura, T., Chauhan, S., Cleyrat, C., & Deretic, V. (2015). Secretory autophagy. *Current Opinion in Cell Biology*, *35*, 106–116.

Poole, K., Schiebel, E., & Braun, V. (1988). Molecular characterization of the hemolysin determinant of *Serratia marcescens*. *Journal of Bacteriology*, *170*, 3177–3188.

Porat-Shliom, N., Milberg, O., Masedunskas, A., & Weigert, R. (2013). Multiple roles for the actin cytoskeleton during regulated exocytosis. *Cellular and Molecular Life Sciences*, *70*, 2099–2121.

Robinson, N., McComb, S., Mulligan, R., Dudani, R., Krishnan, L., & Sad, S. (2012). Type I interferon induces necroptosis in macrophages during infection with *Salmonella enterica* serovar Typhimurium. *Nature Immunology*, *13*, 954–962.

Rodriguez, A., Webster, P., Ortego, J., & Andrews, N. W. (1997). Lysosomes behave as Ca2+-regulated exocytic vesicles in fibroblasts and epithelial cells. *The Journal of Cell Biology*, *137*, 93–104.

Santic, M., Al-Khodor, S., & Abu Kwaik, Y. (2010a). Cell biology and molecular ecology of *Francisella tularensis*. *Cellular Microbiology*, *12*, 129–139.

Santic, M., Pavokovic, G., Jones, S., Asare, R., & Kwaik, Y. A. (2010b). Regulation of apoptosis and anti-apoptosis signalling by *Francisella tularensis*. *Microbes and Infection*, *12*, 126–134.

Schwab, F., Geffers, C., Piening, B., Haller, S., Eckmanns, T., & Gastmeier, P. (2014). How many outbreaks of nosocomial infections occur in German neonatal intensive care units annually? *Infection*, *42*, 73–78.

Silveira, T. N., & Zamboni, D. S. (2010). Pore formation triggered by Legionella spp. is an Nlrc4 inflammasome-dependent host cell response that precedes pyroptosis. *Infection and Immunity*, *78*, 1403–1413.

Sotelo, J., & Benech, J. C. (2013). *Calcium and cellular metabolism: Transport and regulation*. New York: Springer Science & Business Media.

Sridharan, H., & Upton, J. W. (2014). Programmed necrosis in microbial pathogenesis. *Trends in Microbiology*, *22*, 199–207.

Starr, T., Child, R., Wehrly, T. D., Hansen, B., Hwang, S., Lopez-Otin, C., … Celli, J. (2012). Selective subversion of autophagy complexes facilitates completion of the Brucella intracellular cycle. *Cell Host & Microbe*, *11*, 33–45.

Takeuchi, H., Furuta, N., & Amano, A. (2011). Cell entry and exit by periodontal pathogen via recycling pathway. *Communicative & Integrative Biology*, *4*, 587–589.

Thurston, T. L., Wandel, M. P., Von, M. N., Foeglein, A., & Randow, F. (2012). Galectin 8 targets damaged vesicles for autophagy to defend cells against bacterial invasion. *Nature*, *482*, 414–418.

Traven, A., & Naderer, T. (2014). Microbial egress: A hitchhiker's guide to freedom. *PLoS Pathogens*, *10*, .e1004201.

Xu, G., Wang, J., Gao, G. F., & Liu, C. H. (2014). Insights into battles between Mycobacterium tuberculosis and macrophages. *Protein & Cell*, *5*, 728–736.

Yu, V. L. (1979). *Serratia marcescens*: Historical perspective and clinical review. *The New England Journal of Medicine*, *300*, 887–893.

SUPPORTING INFORMATION

Additional Supporting Information may be found online in the supporting information tab for this article.

How to cite this article: Di Venanzio, G., Lazzaro, M., Morales, E. S., Krapf, D., and García Véscovi, E. (2016), A pore-forming toxin enables Serratia a nonlytic egress from host cells, *Cellular Microbiology*, doi: 10.1111/cmi.12656